View metadata, citation and similar papers at core.ac.uk

brought to you by CORE

provided by University of Lincoln Institutional Repository

Biochem. J. (2005) **390**, 19–27 (Printed in Great Britain) doi:10.1042/BJ20050324

Crystal structure of levansucrase from the Gram-negative bacterium *Gluconacetobacter diazotrophicus*

Carlos MARTÍNEZ-FLEITES*†[1], Miguel ORTÍZ-LOMBARDÍA*, Tirso PONS†, Nicolas TARBOURIECH*, Edward J. TAYLOR*, Juan G. ARRIETA‡, Lázaro HERNÁNDEZ‡ and Gideon J. DAVIES*

*Structural Biology Laboratory, Chemistry Department, University of York, York YO10 5YW, U.K., †Physical-Chemistry Division, Center for Genetic Engineering and Biotechnology, PO Box 6162, Havana 10600, Cuba, and ‡Plant Division, Center for Genetic Engineering and Biotechnology, PO Box 6162, Havana 10600, Cuba

The endophytic Gram-negative bacterium *Gluconacetobacter diazotrophicus* SRT4 secretes a constitutively expressed levansucrase (LsdA, EC 2.4.1.10), which converts sucrose into fructo-oligosaccharides and levan. The enzyme is included in GH (glycoside hydrolase) family 68 of the sequence-based classification of glycosidases. The three-dimensional structure of LsdA has been determined by X-ray crystallography at a resolution of 2.5 Å (1 Å = 0.1 nm). The structure was solved by molecular replacement using the homologous *Bacillus subtilis* (*Bs*) levansucrase (Protein Data Bank accession code 1OYG) as a search model. LsdA displays a five-bladed β-propeller architecture, where the catalytic residues that are responsible for sucrose hydrolysis are perfectly superimposable with the equivalent residues of the *Bs* homologue. The comparison of both structures, the mutagenesis data and the analysis of GH68 family multiple sequences alignment show a strong conservation of the sucrose hydrolytic machinery among levansucrases and also a structural equivalence of the *Bs* levansucrase Ca^{2+}-binding site to the LsdA Cys^{339}–Cys^{395} disulphide bridge, suggesting similar fold-stabilizing roles. Despite the strong conservation of the sucrose-recognition site observed in LsdA, *Bs* levansucrase and GH32 family *Thermotoga maritima* invertase, structural differences appear around residues involved in the transfructosylation reaction.

Key words: five-bladed β-propeller, fructosyltransferase, *Gluconacetobacter diazotrophicus*, glycoside hydrolase, glycoside hydrolase 68 family (GH68 family), levansucrase.

INTRODUCTION

Fructans (β-D-fructofuranosyl polymers with a terminal D-glucosyl moiety) constitute the primary carbohydrate reserve in 15 % of higher plants comprising approx. 40 000 species and appear in a wide range of bacterial and fungal species [1]. In plants, fructans are known to be involved in the stabilization of cellular membranes conferring protection from water stress caused by drought or low temperatures [2]. The physiological roles of fructans in bacteria have been less described, and it has been postulated that fructan biosynthesis may be involved in a variety of processes, such as survival of bacteria in soil, phytopathogenesis and symbiosis [3]. Of emerging importance is the use of fructo-oligosaccharides as health-promoting 'pre-biotics', which act as food sources for beneficial bacteria, such as bifidobacteria.

The synthesis of fructans starts with a transfructosylation reaction in which a sucrose molecule plays the role of fructosyl donor and with a second molecule of sucrose the initial acceptor of the fructosyl moiety (Scheme 1). Following initiation, the extension, the type of linkage and the branching of the fructan chain varies according to the enzyme and organism. Fructan synthesis in plants is carried out by the action of two or more FTFs (fructosyltransferases) that are able to produce complex mixtures of fructans with a great variety of linkages of the fructosides [2]. In bacteria, fructan biosynthesis is somewhat simpler because only one multifunctional enzyme is involved. This enzyme is named levansucrase (EC 2.4.1.10) when the product is a fructan of the type levan (β-2,6-linked polyfructan) or inulosucrase (EC 2.4.1.9) when the fructan is of the type inulin (β-2,1-linked polyfructan). Levansucrase catalyses the transfer of the fructosyl residue, from sucrose, to a variety of acceptors including water (sucrose hydrolysis), glucose (exchange), sucrose (oligofructoside synthesis) and fructan (polymerase reaction). The attack of sucrose can occur via O1 to form 1-kestose (1-kestotriose, isokestose; the basis of β-2,1-linked inulins) or via O6 to form the β-2,6-linked fructo-oligosaccharide 6-kestose. These reactions all occur via a Ping Pong mechanism involving the formation of a covalent fructosyl–enzyme intermediate [4–6] (Scheme 1).

Within the sequence-derived classification of GHs (glycoside hydrolases) and transglycosidases [7,8], bacterial FTFs are classified in family GH68 (http://afmb.cnrs-mrs.fr/CAZY) and, recently, the first three-dimensional structure of an FTF was published [9]. FTFs have also been shown to be structurally similar to sucrose-6-phosphate hydrolases, invertases, fructanases and eukaryotic FTFs found in family GH32. Together GH68 and GH32 thus comprise the β-fructofuranosidase clan GH-J.

The recent crystal structure of Gram-positive bacterium *Bacillus subtilis* (hereafter *Bs*) levansucrase and its complex with sucrose revealed the structural determinants for substrate recognition and the spatial disposition of three key catalytic acidic residues at the active site. The structure displays a five-bladed β-propeller topology that is shared with the elucidated crystal structures of *Thermotoga maritima* invertase (GH32) [10], *Cellvibrio japonicus* α-L-arabinanase (GH43) [11] and the *Cichorium intybus* fructan 1-exohydrolase IIa (GH32) [12]. Despite their high degree of structural similarities in the disposition of catalytic residues at the active site, the GH43 α-L-arabinanase operates with

Abbreviations used: *Bs*, *Bacillus subtilis*; FTF, fructosyltransferase; *Gd*, *Gluconacetobacter diazotrophicus*; GH, glycoside hydrolase; NCS, non-crystallographic symmetry; R.M.S.D., root mean square deviation.

[1] To whom the correspondence should be addressed (email martinez@ysbl.york.ac.uk).

Atomic co-ordinates and structure factor file have been deposited with the Protein Data Bank (accession code 1W18).

© 2005 Biochemical Society

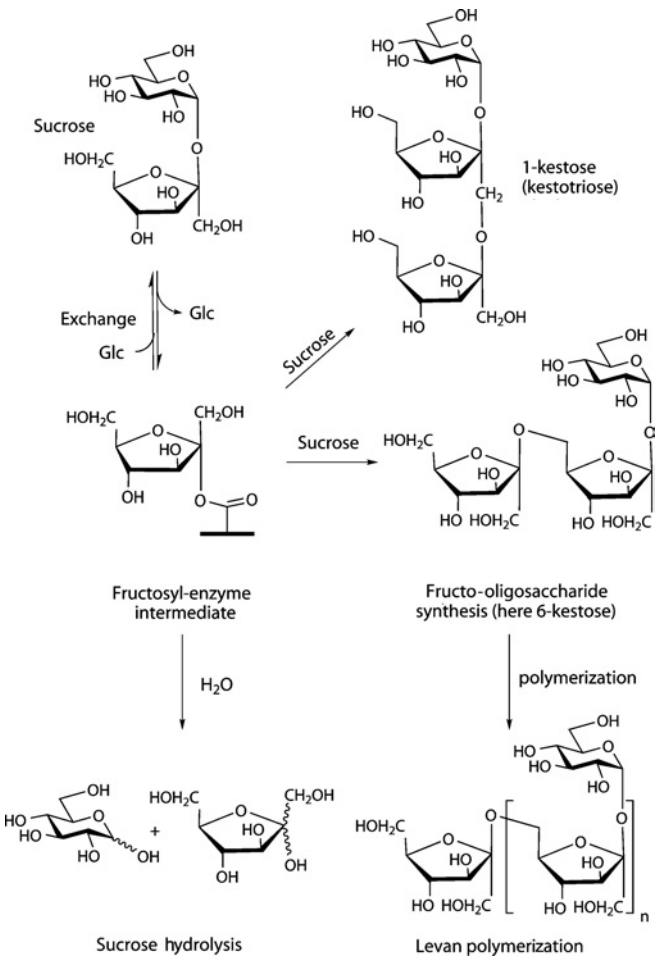

Scheme 1 Various reactions catalysed by levansucrase

inversion of the anomeric configuration of the substrate, while levansucrases and invertases are 'retaining' enzymes.

The endophytic Gram-negative bacterium *Gluconacetobacter diazotrophicus* (hereafter *Gd*) secretes a constitutively expressed levansucrase (LsdA), which is responsible for utilization of the natural substrate sucrose [5,13]. The kinetic parameters of the levansucrases from the *Bs* and *Gd* are of the same order of magnitude in the initial step of the reaction, the formation of the fructosyl–enzyme intermediate, but there are remarkable differences in the affinity of the intermediates for the various fructosyl acceptors [5,14]. *Bs* levansucrase catalyses the formation of high-molecular-mass levan without accumulation of transient oligofructans, whereas *Gd* levansucrase synthesizes and accumulates a large amount of β-2,1-linked tri- and tetra-saccharides, with a much lower yield of levan under the same reaction conditions [5]. The structural determinants for the polymerization reaction of FTFs remain at present poorly understood, not least because a single structure makes it hard to mine the 48 (as of 25 April 2005) GH68 family members. The combined analysis of protein sequences, mutagenesis data and three-dimensional structures of levansucrases with different catalytic performances should thus contribute to a deeper insight into the polymerization mechanism of FTFs. In the present paper, as part of this process, we report the crystal structure of *Gd* levansucrase at a resolution of 2.5 Å (1 Å = 0.1 nm) in its ligand-free state and limited biochemical analyses to support a detailed comparison with its *Bs* homologue.

MATERIALS AND METHODS

Bacterial strains and media

Escherichia coli strains DH5α [Φ80d*lacZ*ΔM15 *recA*1 *endA*1 *gyrA*96 *thi*-1 *hsdR*17 (r_K^- m_K^+) *supE*44 *relA*1 *deoR* Δ(*lacZYA-argF*)U169] and S17-1 {*thi pro hsd*R *rec*A [RP4-2(Tc::Mu)(Km::Tn7)]} [15] were used as a cloning host and as a conjugative donor host respectively. *E. coli* strains were grown at 37 °C in Luria–Bertani broth supplemented with ampicillin (50 μg/ml) and tetracycline (12.5 μg/ml) when needed. *Gd* strains SRT4 (wild-type, Lev^+) and AD5 (SRT4 *lsdA*::*nptII-ble* cassette, Lev^-) [16] were grown at 28 °C in LGIE medium containing 5 % (w/v) sucrose and 1 % (v/v) glycerol [17]. Chloramphenicol (30 μg/ml) and tetracycline (20 μg/ml) were added to LGIE agar medium to select the transconjugants.

Site-directed mutagenesis

Plasmid pALS137 carries the 3.2-kb HindIII/NruI fragment from plasmid pALS5 [17] inserted into pUC8 digested with HindIII/SmaI. Plasmid pALS137 containing the levansucrase gene (*lsdA*) under its own promoter was used as template for mutagenesis using the GeneEditor Kit (Promega). The oligonucleotides 5′-GATGTCTGGGTCTGG**A**ACACGTGGACCC-TGATCGAC-3′, 5′-CCAGCGTGGCGTCGCGAAC**A**GCACC-GAGGCCGATC-3′ and 5′-CTGATTTCGGCCAACA**C**GCGTCA-ATGATCAGACCGAACGGCCG-3′ were used to generate the mutations D135N, C339S and C395S respectively (amino acid substitutions are in bold, restriction sites created by silent mutations are underlined). Plasmids from *E. coli* transformants resistant to the GeneEditor Antibiotic Selection Mix were screened by digestion with PmlI (D135N), NruI (C339S) and BclI (C395S), and mutations were confirmed by DNA sequencing. The plasmids carrying the mutations D135N, C339S and C395S in the *lsdA* gene were named pALS191, pALS201 and pALS203 respectively.

Enzyme expression in lsdA::nptII-ble *Gd* mutant

Plasmids pALS137, pALS190, pALS201 and pALS203 were HindIII-linearized and inserted into the broad-range cloning vector pRK293 [18]. The resulting plasmids were named pALS148, pALS192, pALS205 and pALS207 respectively and were used to transform *E. coli* S17-1 (*tra*$^+$). The conjugal mating procedure as described by Arrieta et al. [17] was used to mobilize plasmids pALS148, pALS192, pALS205 and pALS207 into the *Gd* mutant AD5, in which the *lsdA* gene is replaced by the *nptII-ble* cassette.

Crystallization, data collection and refinement

Details of protein expression, purification and crystallization were as reported previously [19]. Crystals grew over 2 weeks using ammonium sulphate in the range 0.35–0.6 M in 0.1 M sodium citrate, pH 5.6, with 30–60 % ethanol and the detergents SDS (1.5–5.0 mM) and β-octylglucoside (10–40 mM) present. Handling crystals grown in $\sim$50 % ethanol was extremely difficult and approx. 50 crystals had to be screened in order to gain a single ordered specimen for data collection. A 2.5 Å resolution dataset was collected from a single crystal at 100 K on beamline ID14-EH1 [ESRF (European Synchrotron Radiation Facility), Grenoble, France] using an ADSC Quantum-4 detector. Diffraction images were integrated with MOSFLM and scaled and reduced with SCALA from the CCP4 suite of programs [20]. Data collection statistics are summarized in Table 1. The structure was solved by molecular replacement using the co-ordinates of *Bs* levansucrase as a search model (Protein Data Bank accession code 1OYG) with all residues (except alanine and glycine) truncated

© 2005 Biochemical Society

Table 1 Summary of data collection and refinement statistics

Values in parentheses refer to the highest resolution shell, 2.64–2.5 Å, for the final dataset. $R_{sym} = \Sigma(I - \langle I \rangle)^2/\Sigma I^2$.

Parameter	Value
Data collection	
High resolution (Å)	2.5
Completeness (%)	99.2 (98.5)
Multiplicity	3.3 (3.2)
R_{sym}	0.078 (0.318)
$\langle I/\sigma I \rangle$	11.6 (4.6)
Refinement	
Resolution used in refinement (Å)	105.4–2.5
Total number of non-hydrogen atoms	7848
Number of water molecules	194
Number of sulphate ions	4
R_{cryst} (%)	19.6
R_{free} (%)*	24.9
Average *B*-factor	
Protein atoms (Å^2)	25.7
Sulphate ions atoms (Å^2)	74.3
Solvent atoms (Å^2)	34.1
R.M.S.D. from ideal values†	
Bond lengths (Å)	0.014
Bond angles (°)	1.51
B-factor for bonded atoms	
Main chain bonds (Å^2)	0.612
Main chain angles (Å^2)	0.786
Side chain bonds (Å^2)	1.232
Side chain angles (Å^2)	1.920
Protein Data Bank accession code	1W18

* R_{free} calculated using 5 % of total reflections omitted from refinement.
† Data from [45].

to serine. The program AMoRe [21] was used with data in the resolution range 20–4 Å and an outer radius of Patterson integration of 37 Å.

For refinement, 5 % of the observations were set aside for cross-validation analysis [22] and were used to monitor various refinement strategies. Simulated annealing by slow cooling and positional refinements were initially performed on the molecular replacement solution with CNS [23] using NCS (non-crystallographic symmetry) restraints. CNS density modification procedures and 2-fold map averaging were applied to the calculated 2Fo-Fc maps, and this allowed the placement of the structurally most conserved residues. After several cycles of NCS refinement with NCSref [20] interspersed with cycles of manual building with Xfit [24], it was possible to place approx. 70 % of the residues. Using phases calculated from this incomplete model, ARP/wARP [20] built approx. 90 % of the residues as serine, valine, alanine and glycine that were later mutated to the correct side chains. The rest of the residues, mainly in loop regions, were placed manually with Xfit [24]. Final refinement cycles were performed with REFMAC [25] using NCS restraints and TLS (translation, libration and screw-rotation) corrections [26]. Water molecules and four sulphate ions were placed at peak positions of σ_a-weighted [27] Fo-Fc maps and 2Fo-Fc maps greater than 3σ and 1σ respectively and were checked at the graphic display. A summary of refinement statistics is shown in Table 1. The final model was validated against composite annealed omit maps from CNS. Ramachandran [28] statistics produced by PROCHECK [29] indicate that 82.9 % of the residues are located in the most favoured regions of the plot and 16.1 % in additional allowed regions. Eight residues were found in generous allowed regions with no residues located in the disallowed regions. Co-ordinates have been deposited at the Protein Data Bank [30] under accession code 1W18.

RESULTS AND DISCUSSION

Structure of *Gd* levansucrase LsdA

The open reading frame of *Gd* levansucrase (LsdA) encodes a 584-residue protein with a 30-residue N-terminal signal peptide that is cleaved off during secretion. The mature protein thus comprises a 553-residue polypeptide (numbering 31–584) with an N-terminal pyroglutamate. LsdA contains three cysteine residues (Cys^{157}, Cys^{339} and Cys^{395}), with Cys^{339} and Cys^{395} engaged in a disulphide bridge [31].

The crystal structure of LsdA (residues 62–554) was solved by molecular replacement using the homologous *Bs* levansucrase [9] as the search model at a resolution of 2.5 Å and was subsequently refined to crystallographic *R*-factors of 19.6 % (R_{cryst}) and 24.9 % (R_{free}) (Table 1). The asymmetric unit contains two copies of the polypeptide chain, and, in addition, 194 water molecules and four sulphate ions have been modelled. Tight NCS restraints were maintained throughout the refinement and model-building harnessed electron density maps averaged according to the co-ordinate-derived NCS operators.

LsdA displays the five-bladed β-propeller fold (Figure 1), as first reported for the N-acetylglucosamine-binding tachylectin [32] and as first observed as an enzyme fold for the GH43 arabinanase [11] and then subsequently for the invertase from *T. maritima* [10] and the fructan 1-exohydrolase from *Ci. intybus* [12]. The five β-sheet modules are arranged in consecutive order with 5-fold pseudosymmetry around a central cavity. As in other β-propellers described so far, the four β-strands composing each β-sheet display a strong twist with an average of 90° between the first and the last strand. Similarly to *Bs* levansucrase and arabinanase, LsdA does not possess 'molecular Velcro', a term colloquially used to describe the closure of the propeller fold in which the N-terminal first strand forms the outermost β-strand of the C-terminal blade [33,34]. Fold stabilization is, however, provided by the packing of the N- and C-termini of the polypeptide. As in *Bs* levansucrase, the LsdA N-terminus runs along the perimeter of blade IV forming a clamp-like loop that adds a fifth β-strand to blade III (numbered as βIIIE in Figure 2). Additionally in LsdA, the N-terminus (residues 76–78) forms a short two-stranded antiparallel β-sheet that extends to a β-strand (residues 442–444) located in the insertion between βIVC and βIVD (β-strands numbered as β1 and β4). Different from *Bs* levansucrase, the C-terminus in LsdA does engage in hydrogen-bonding interactions to the central core through the formation of a two-stranded parallel β-sheet between β-strand 2 (residues 147–150) and β-strand 5 (residues 542–545).

Comparison with the *Bs* levansucrase

LsdA presents an overall sequence identity with its *Bs* homologue of 26 %, but, in the 283 structurally equivalent residues, the sequences share 31 % identity. The secondary-structure elements superimpose well, with an R.M.S.D. (root mean square deviation) of 1.24 Å over 283 equivalent Cα atoms. Not surprisingly, greater variation is observed in insertions into surface loops, a feature commonly found in the β-propeller fold [35]. Several helices, including short stretches of 3_{10}-helix, are conserved along the sequence alignment (Figure 2). In both structures, the longest insertion is found between β-strands IIIB and IIIC, where three helical stretches are interspersed.

LsdA contains a disulphide bridge (Cys^{339}–Cys^{395}) that links the extended loop between β-strands IIIB and IIIC with the insertion

© 2005 Biochemical Society

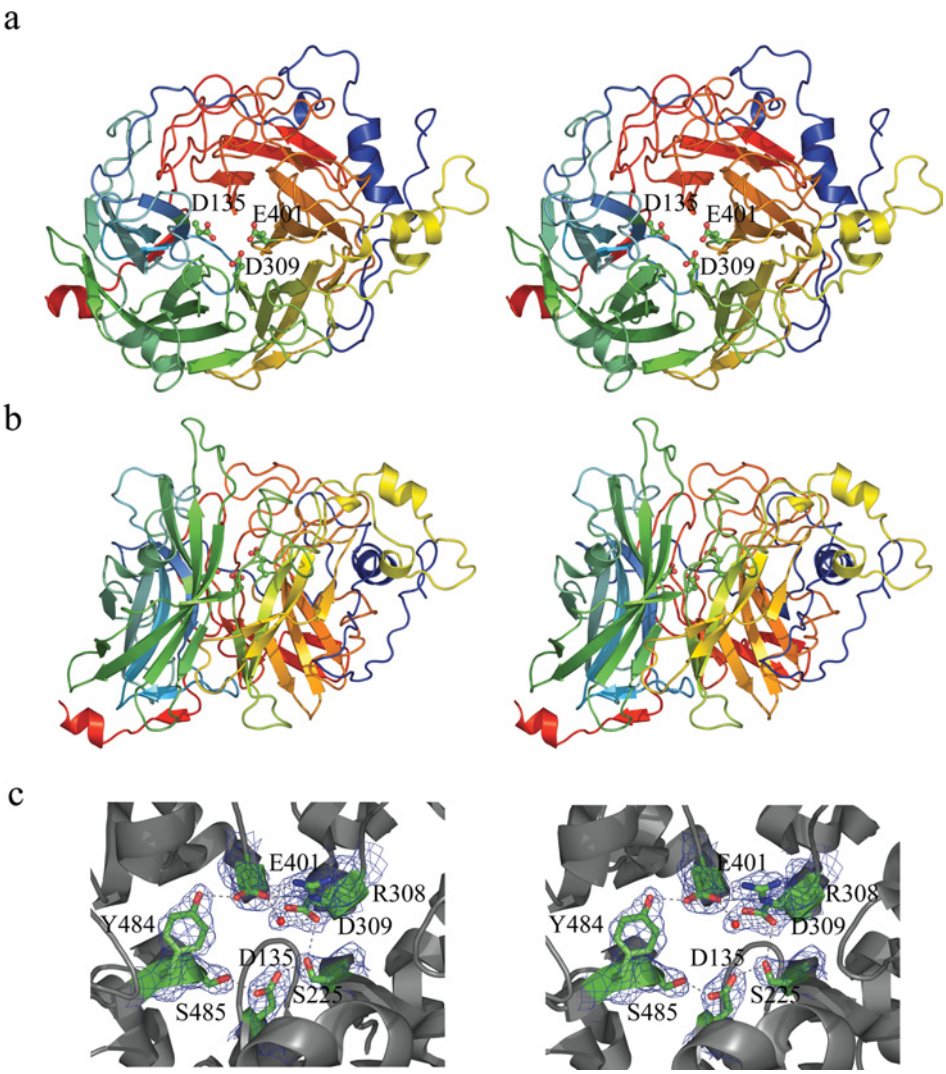

Figure 1 Three-dimensional structure of LsdA

Superior (**a**) and lateral (**b**) stereo views of the five-bladed β-propeller fold. The colour is 'ramped' from N- (blue) to C- (red) terminus. Catalytic residues Asp^{135}, Asp^{309} and Glu^{401} are shown in ball-and-stick representation. (**c**) Stereo view of the electron density map (contoured at 1σ level) 'carved' around catalytic residues and other residues involved in the hydrogen-bond (broken lines) network at the active site. These Figures were prepared with PYMOL [47].

located between blades III and IV. The replacement of either Cys^{339} or Cys^{395} by serine reduced the k_{cat} for sucrose hydrolysis approx. 60-fold (Table 2). Although equivalent cysteine residues appear in the levansucrases from the high-GC content Gram-positive species *Arthrobacter* sp. K-1 (GenBank® accession number BAB72022) and *Actinomyces naeslundii* (GenBank® accession number AAG09737) and the Gram-negative species *Burkholderia cepacia* R1808 (GenBank® accession number ZP_00218900) and *Burkholderia pseudomallei* K96243 (GenBank® accession number YP_110564), there is no general conservation of this disulphide bridge among GH68 family members. Indeed, a pair of cysteine residues is absent in most Gram-positive FTFs, including *Bs* levansucrase. Levansucrases from Gram-negative bacteria *Rahnella aquatilis*, *Pseudomonas syringae* and *Pseudomonas aurantica* display two highly conserved cysteine residues elsewhere, which are not equivalent to those found in LsdA and that might also be implicated in a disulphide bridge. It has been reported that the incubation with dithiothreitol or 2-mercaptoethanol decreased the enzyme activity of *Ps. syringae* levansucrase [36]. In *Zymomonas mobilis* levansucrase the substitution of serine for cysteine residues 121, 151 and 244 abolished the levan-forming activity and halved the sucrose hydrolysis activity [37]. In contrast, *Bs* levansucrase contains a Ca^{2+} ion connecting residues Asp^{241}, Gln^{272}, Leu^{308} and Asn^{310} located in the longest insert between β-strands IIIB and IIIC, with Asp^{339} placed in the insertion between blades III and IV. Leu^{308} is not found strictly conserved in Gram-positive levansucrases, possibly due to the fact that the Ca^{2+} interaction with this residue is through the backbone carbonyl oxygen. The residues involved in Ca^{2+} binding are strictly conserved among FTFs from Gram-positive bacteria, except the high-GC content species *Ac. naeslundii* and *Arthrobacter* sp., but variable in the levansucrases of Gram-negative bacteria (see partial alignment in Figure 3). Thus the activity of LsdA and other levansucrases from Gram-negative bacteria is not affected in the presence of metal ions, such as Ca^{2+}, or the chelating agent EDTA [5,37,38]. In contrast, FTFs from the Gram-positive species *Streptococcus mutans* [39], *Streptococcus salivarius* [6] and *Lactobacillus reuteri* [40,41] show maximal activity only upon addition of 1 mM Ca^{2+}. The fact that both the disulphide bridge in LsdA and the Ca^{2+}-binding site in *Bs*

© 2005 Biochemical Society

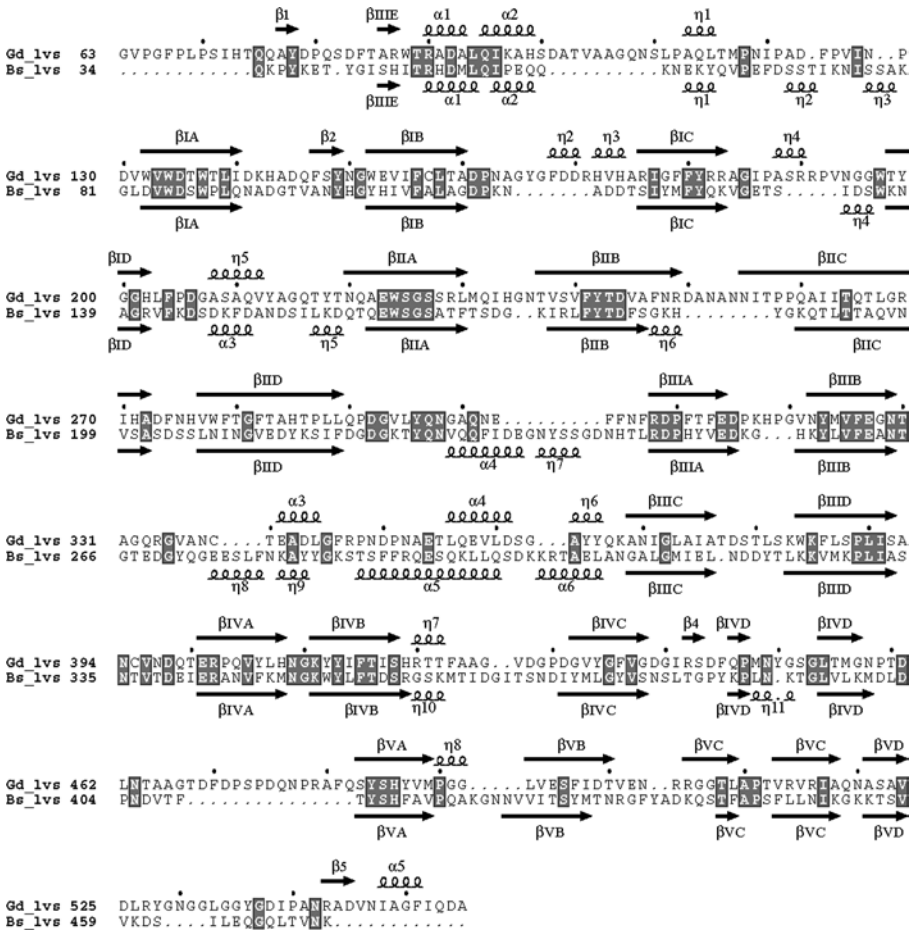

Figure 2 LsdA (Gd_lvs) and *Bs* levansucrase (Bs_lvs) sequence alignment based on structural superimposition generated by TOP [20]

Secondary-structural elements were assigned using DSSP [48] and are indicated by arrows (β-strands) and squiggles (helices). These elements were labelled following the *Bs* levansucrase numbering in [9]. A roman numeral (I–V) is assigned to each β-sheet module, and, in each module, the β-strands are numbered with a capital letter (A–D). α- and 3_{10}-helices (labelled α and η respectively) are numbered consecutively. Strictly conserved residues are boxed. The Figure was produced with ESPript [49].

Table 2 Kinetic parameters of wild-type and site-directed mutant enzymes

The native and mutant enzymes were purified from culture supernatants as described by Arrieta et al. [17] and quantified by the Bradford procedure using BSA as a standard. The reaction mixtures (50 μl) containing 200 mM sucrose in 0.1 M sodium acetate, pH 5.0, were incubated with 0.3 unit of purified enzyme at 30 °C. After 15 min, the reaction was stopped by heating in a boiling-water bath for 5 min. Glucose released from sucrose hydrolysis was measured by a glucose oxidase/peroxidase-coupled colorimetric reaction. The k_{cat} was calculated using 60 000 as the M_r of a functional unit of levansucrase. The K_m for sucrose was determined within a substrate concentration range 1–150 mM at 30 °C and pH 5.0. The kinetic parameters were determined by non-linear regression analysis of substrate–velocity plots using the LEONORA program [46]. One unit of enzyme activity is defined as the amount of enzyme releasing 1 μmol of glucose/min based on initial-velocity measurements under the following conditions: 0.2 M sucrose in 0.1 M sodium acetate buffer, pH 5.0, at 30 °C. Values are means $\pm$ S.D. ($n = 6$).

Strain	Mutation	k_{cat} (min^{-1})	K_m (mM)	k_{cat}/K_m (M^{-1} · min^{-1})
AD5 (pALS148)	Wild-type	$(3.9 \pm 0.2) \times 10^3$	11.9 ± 0.4	3.3×10^5
AD5 (pALS192)	D135N	1.7 ± 0.2	12.3 ± 0.9	1.4×10^2
AD5 (pALS205)	C339S	66.9 ± 2.3	13.8 ± 1.2	4.8×10^3
AD5 (pALS207)	C395S	71.8 ± 6.4	13.1 ± 1.4	5.5×10^3

levansucrase map in structurally equivalent regions in their respective molecular architectures suggests that these features play a similar role in structural maintenance of the catalytic glutamate residue (Glu^{401} in LsdA and Glu^{342} in *Bs* levansucrase), found in the highly conserved 'D(E/Q)(T/I/V)ER' motif, poised for catalysis [9].

The active site of LsdA

Three strictly conserved acid residues have been identified in alignments of protein sequences corresponding to GH families 32, 43, 62 and 68 [42] (boxed residues in Figure 3). Site-directed mutagenesis of these carboxy residues has been performed for various representatives of GH68. On the basis of the mutagenesis and the structural information, it has been proposed that acidic residues Asp^{135}, Asp^{309} and Glu^{401} of LsdA act as the catalytic nucleophile, the 'transition-state stabilizer' and the general acid–base catalyst respectively. Substitution of asparagine for Asp^{135} resulted in an enzyme with substantially impaired activity, with a 2300-fold decrease in k_{cat} (Table 2). It has also been reported that mutation of Asp^{309} to asparagine in the RPD (Arg-Pro-Asp) motif reduced the k_{cat} 75-fold, again without change in the K_m [38].

In the crystal structure of LsdA, the catalytic constellation of carboxy residues is located at the bottom of a funnel-shaped cavity at the centre of the β-propeller (Figure 1). Each one of these residues, namely Asp^{135}, Asp^{309} and Glu^{401}, belong to the first and innermost β-strand of blades I, III and IV respectively. This feature is commonly found in this type of fold, where the surface of the central cavity is mostly lined by residues that belong to the

© 2005 Biochemical Society

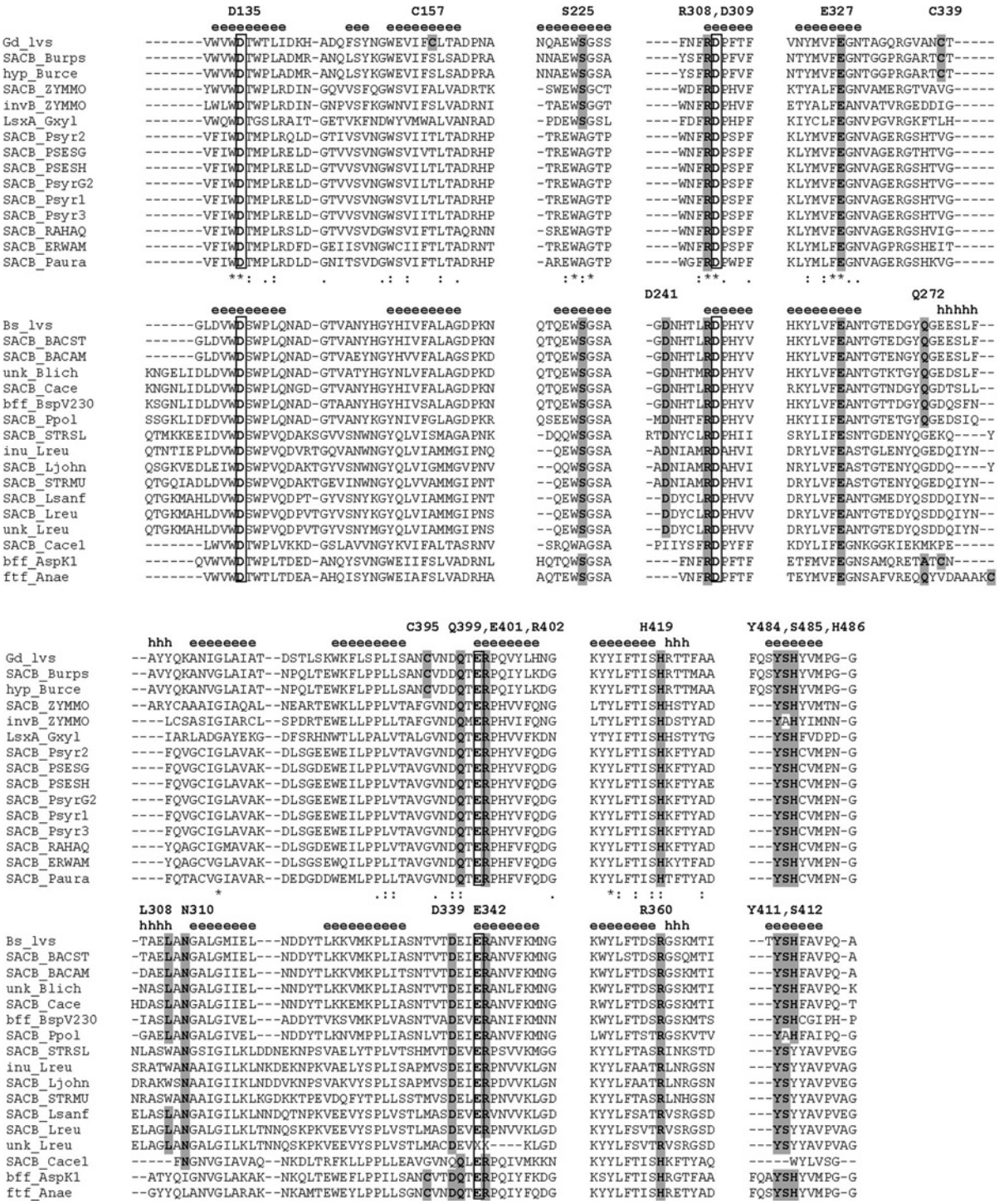

Figure 3 Multiple sequence alignment of selected fragments of GH68 family members

The sequences are divided into two groups, Gram-negative and Gram-positive levansucrases headed by LsdA (Gd_lvs) and *Bs* levansucrase (Bs_lvs) respectively. Protein identifiers and access codes for each sequence in the SwissProt/TrEMBL and GenBank® databases are as follows: *Gd* LsdA (Gd_lvs, Q43998); *B. pseudomallei* K96243 levansucrase (SACB_Burps, YP_110564); *B. cepacia* R1808 hypothetical protein (hyp_Burce, ZP_00218900); *Z. mobilis* levansucrase (SACB_ZYMMO, Q60114, Q06487, Q60116), and invertase (invB_ZYMMO, AAA61488); *Gluconacetobacter xylinus* levansucrase (LsxA_Gxyl, BAA93720); *Ps. syringae* pv. *tomato* levansucrase (SACB_Psyr1, AAO54974; SACB_Psyr2, AAO55819; SACB_Psyr3, AAO59056); *Ps. syringae* pv. *glycinea* levansucrase (SACB_PSESG, O52408; SACB_PsyrG2, AAK49952); *Ps. syringae* pv. *phaseolicola* levansucrase (SACB_PSESH, O68609); *R. aquatilis* levansucrase (SACB_RAHAQ, O54435); *Erwinia amylovora* levansucrase (SACB_ERWAM, Q46654); *Ps. aurantiaca* levansucrase (SACB_Paura, AAL09386); *Bs* levansucrase (Bs_lvs, P05655, P70984); *Bacillus stearothermophilus* levansucrase (SACB_BACST, P94468); *Bacillus amyloliquefaciens* levansucrase (SACB_BACAM, P21130); *Bacillus licheniformis* unnamed protein product (unk_Blich, CAF05486); *Clostridium acetobutylicum* levansucrase (SACB_Cace, CAC1772; SACB_Cace1, CAC1774); *Bacillus* sp. V230 β-fructofuranosidase (bff_BspV230, BAA32083); *Pa. polymyxa* levansucrase (SACB_Ppol, CAB39327); *Streptococcus salivarius* levansucrase (SACB_STRSL, Q55242); *L. reuteri* inulosucrase (inu_Lreu, AAN05575), levansucrase (SACB_Lreu, AAO14618) and unnamed protein product (unk_Lreu, CAD19335); *Lactobacillus johnsonii* levansucrase (SACB_Ljohn, NP_964768); *Streptococcus mutans* levansucrase (SACB_STRMU, P11701); *Lactobacillus sanfranciscensis* levansucrase (SACB_Lsanf, CAD48195); *Arthrobacter* sp. K-1 β-fructofuranosidase (bff_AspK1, BAB72022); *Ac. naeslundii* FTF (ftf_Anae, AAG09737). Secondary-structural elements were assigned using DSSP [48] and are indicated by 'e' (β-strands) and 'h' (helices). Catalytic residues Asp[135], Asp[309] and Glu[401] are boxed.

© 2005 Biochemical Society

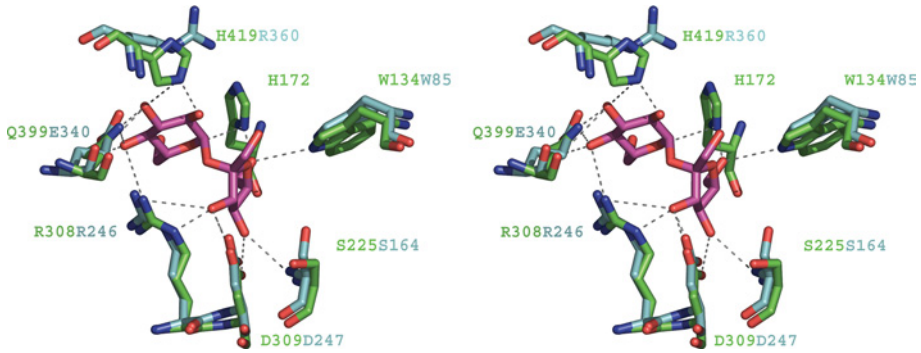

Figure 4 Sucrose-binding site of LsdA

The Figure shows an overlap of the co-ordinates of the *Bs* levansucrase E342A -sucrose complex (Protein Data Bank accession code 1PT2) with the *Gv* levansucrase, LsdA. Potential hydrogen-bonding interactions are represented by broken lines. LsdA residues are bond-coloured green and *Bs* levansucrase are turquoise. Labels of depicted residues follow the same colour pattern.

first strand of each modular sheet [35]. The three carboxylic residues in LsdA are perfectly superimposable on to the equivalent residues in *Bs* levansucrase and are spaced some 4.8–7.4 Å from each other. The proposed catalytic nucleophile, Asp^{135}, side chain forms two hydrogen bonds with side chains of Ser^{225} and Ser^{485} (Figure 1c); the same pattern of interactions is present in *Bs* levansucrase for the equivalent residue. Both serine residues are found highly conserved in the GH68 family multiple sequence alignment, except that the equivalent to Ser^{225} in some of the Gram-negative bacteria, including *Pseudomonas*, *Rhanella* and *Erwinia* species, have an alanine residue in this position (Figure 3). Interestingly, the LsdA motif Tyr^{484}-Ser^{485}-(His/Tyr/Trp)^{486} is strictly conserved in GH68 family, except in *Z. mobilis* invertase and *Paenibacillus polymyxa* levansucrase, where Ser^{485} is found replaced by alanine. The structurally equivalent residues of LsdA Ser^{485} and *Bs* levansucrase Ser^{412} in *T. maritima* invertase and *Ci. intybus* fructan 1-exohydrolase are Ala^{241} and Ala^{275} respectively, and, in the multiple sequence alignment of the GH32 family, an alanine residue is found highly conserved in this position (this motif was described as motif F in [43]). The high conservation of serine in this position in GH68 levansucrases and its replacement by alanine in GH32 invertases, levanases or sucrases suggests that this H-bond interaction could play an important role in the orientation of the nucleophilic residue during transfructosylation catalysis.

The side chain of Asp^{309} forms hydrogen bonds to Ser^{225}, the Arg^{402} backbone amide nitrogen and a water molecule that, at the same time, forms a hydrogen bond with the catalytic residue Glu^{401}. The Glu^{401} side chain in turn establishes hydrogen bonds with side chains of Glu^{327} and Tyr^{484} and a salt bridge with Arg^{308} (Figure 1c). The equivalent positions of LsdA Arg^{308} and Tyr^{484} are found strictly conserved in GH68 family and are also conserved in GH32 family members (described as motifs D and F in [43]). The LsdA equivalent Glu^{327} position is strictly conserved in GH68 family, but is highly variable in representatives of GH32 family.

Analysis of the sucrose complex of the inactive mutant of *Bs* levansucrase (Protein Data Bank accession code 1PT2) [9] revealed the residues involved in substrate recognition. All of these residues, except for Gln^{399}/Glu^{340} and His^{419}/Arg^{360} (LsdA/*Bs* levansucrase numbering), are present in LsdA. Indeed, structural overlap of this subset of co-ordinates gives a R.M.S.D. of 0.75 Å for the Cα atoms of residues that are responsible for sucrose recognition and catalysis. This close similarity allows the modelling and analysis of contacts of the sucrose molecule at the active site in LsdA. Figure 4 shows the LsdA sucrose-binding site and the potential hydrogen-bonding interactions of the sucrose molecule with LsdA based on the actual interactions with *Bs* levansucrase inactive mutant (Protein Data Bank accession number 1PT2). Most of the hydrogen-bonding interactions observed in the *Bs* levansucrase sucrose complex appear to be conserved in the modelled interaction of sucrose and LsdA. This high degree of structural conservation at the sucrose-binding site is in agreement with the enzymatic data that report kinetic constants of the same order of magnitude for the initial step of the transfructosylation reaction [5], i.e. the formation of the fructosyl–enzyme intermediate, and the overall sucrose hydrolysis reaction (Table 3). In addition, the residues involved in the hydrogen-bond network of interactions at the sucrose hydrolysis active site are found strictly conserved in the GH68 sequence alignment (Figure 3).

Table 3 Apparent kinetic constants for the *Bs* and *Gd* levansucrases (adapted from [5])

Values are given for the (forward) rate of intermediate formation (k_{+2}) and subsequent hydrolysis, levan (lev) production and inulin (inu) production. Under conditions of 1 M sucrose, the *Gd* enzyme transfers approx. one-third of the fructosyl–enzyme intermediate to sucrose to form 1-kestose. Such a reaction was not observed for the *Bs* enzyme.

Origin	k_{+2} (s^{-1})	$k_{hydrolysis}$ (s^{-1})	k_{lev} ($M^{-1} \cdot s^{-1}$)	k_{inu} ($M^{-1} \cdot s^{-1}$)
Gd	550	51	1×10^4	Not detected
Bs	260	35	4×10^4	7×10^3

The sucrose hydrolytic machinery is located at the bottom of the catalytic pocket, and the residues that line this zone are located in the first β-strand of each blade. Immediately above this zone and surrounding the modelled glucosyl moiety of the sucrose molecule, it is possible to describe a fringe of residues that belong to the inserts that link β-strand B with C in each blade (see Figure 4). His^{419} of LsdA is located in this region and is the structural equivalent of *Bs* levansucrase Arg^{360} and the sequence equivalent of *Z. mobilis* levansucrase His^{296}. Indeed, in Gram-negative levansucrases, a histidine residue is found strictly conserved in the equivalent position of LsdA His^{419}, while in Gram-positive representatives an arginine residue is present (see the alignment in Figure 3). In both LsdA and *Bs* levansucrase, a tyrosine residue, whose aromatic ring is placed parallel to the plane of the histidine ring or the guanidinium group in LsdA His^{419} or *Bs* levansucrase Arg^{360} (Tyr^{484} in LsdA and Tyr^{411} in *Bs* levansucrase) is found

© 2005 Biochemical Society

strictly conserved in all levansucrases. Both *Bs* levansucrase Arg^{360} and *Z. mobilis* levansucrase His^{296} are reported to be crucial for the catalysis of the transfructosylation reaction [14,44], suggesting that a positively charged and electron delocalizing environment is required around this position. This suggestion is supported further by the fact that *T. maritima* invertase [10] does not have a structural equivalent residue to LsdA His^{419} or *Bs* levansucrase Arg^{360}, and *Ci. intybus* fructan 1-exohydrolase shows a glutamate residue (Glu^{234}) pointing in the opposite direction to *Bs* levansucrase Arg^{360} [12]. The presence of residual transfructosylation activity in *Bs* levansucrase $Arg^{331} \rightarrow$ Ser/Leu mutants [14] also indicates that the structural determinants for the transfructosylation catalysis are more complex and at present not fully understood. Indeed, the absence of structural data for complexes between fructosyl acceptors and levansucrases makes it difficult to reach conclusions about what determines the outcome of the transfructosylation reaction in which LsdA releases large amount of 1-kestotriose (Glc- and kestotetraose in the initial phase of the reaction [5]), while *Bs* levansucrase synthesizes long-chain fructans under similar reaction conditions (Table 3). The crystallographic structures currently available of members of GH68 and GH32 families, together with the sequences and biochemical data, strongly support the hypothesis that FTFs evolved from invertases through comparatively small mutational events [2]. The LsdA structure presented in the present paper sheds some light on some of these changes and should help inform subsequent mutagenesis experiments in order to explore and harness the structural determinants that are responsible for transfructosylation.

We thank Professor Guy Dodson from the National Institute for Medical Research in London and the Chemistry Department, University of York for his support on this project. Collaboration between C.M.-F. and the University of York was made possible through funding from the Royal Society. G.J.D. is a Royal Society University Research Fellow.

REFERENCES

1 Cairns, A. J. (2003) Fructan biosynthesis in transgenic plants. J. Exp. Bot. **54**, 549–567

2 Vijn, I. and Smeekens, S. (1999) Fructan: more than a reserve carbohydrate? Plant Physiol. **120**, 351–360

3 Cote, G. L. and Ahlgren, J. A. (1993) Metabolism in microorganisms, part I: levan and levansucrase. In Science and Technology of Fructans (Suzuki, M. and Chatterton, N. J., eds.), pp. 141–168, CRC Press, Boca Raton

4 Chambert, R., Treboul, G. and Dedonder, R. (1974) Kinetic studies of levansucrase of *Bacillus subtilis*. Eur. J. Biochem. **41**, 285–300

5 Hernandez, L., Arrieta, J., Menendez, C., Vazquez, R., Coego, A., Suarez, V., Selman, G., Petit-Glatron, M. F. and Chambert, R. (1995) Isolation and enzymic properties of levansucrase secreted by *Acetobacter diazotrophicus* SRT4, a bacterium associated with sugar cane. Biochem. J. **309**, 113–118

6 Song, D. D. and Jacques, N. A. (1999) Purification and enzymic properties of the fructosyltransferase of *Streptococcus salivarius* ATCC 25975. Biochem. J. **341**, 285–291

7 Henrissat, B. (1991) A classification of glycosyl hydrolases based on amino acid sequence similarities. Biochem. J. **280**, 309–316

8 Henrissat, B. and Davies, G. (1997) Structural and sequence-based classification of glycoside hydrolases. Curr. Opin. Struct. Biol. **7**, 637–644

9 Meng, G. and Futterer, K. (2003) Structural framework of fructosyl transfer in *Bacillus subtilis* levansucrase. Nat. Struct. Biol. **10**, 935–941

10 Alberto, F., Bignon, C., Sulzenbacher, G., Henrissat, B. and Czjzek, M. (2004) The three-dimensional structure of invertase (β-fructosidase) from *Thermotoga maritima* reveals a bimodular arrangement and an evolutionary relationship between retaining and inverting glycosidases. J. Biol. Chem. **279**, 18903–18910

11 Nurizzo, D., Turkenburg, J. P., Charnock, S. J., Roberts, S. M., Dodson, E. J., McKie, V. A., Taylor, E. J., Gilbert, H. J. and Davies, G. J. (2002) *Cellvibrio japonicus* α-L-arabinanase 43A has a novel five-blade β-propeller fold. Nat. Struct. Biol. **9**, 665–668

12 Verhaest, M., Ende, W. V., Roy, K. L., De Ranter, C. J., Laere, A. V. and Rabijns, A. (2005) X-ray diffraction structure of a plant glycosyl hydrolase family 32 protein: fructan 1-exohydrolase IIa of *Cichorium intybus*. Plant J. **41**, 400–411

13 Hernandez, L., Sotolongo, M., Rosabal, Y., Menendez, C., Ramirez, R., Caballero-Mellado, J. and Arrieta, J. (2000) Structural levansucrase gene (lsdA) constitutes a functional locus conserved in the species *Gluconacetobacter diazotrophicus*. Arch. Microbiol. **174**, 120–124

14 Chambert, R. and Petit-Glatron, M. F. (1991) Polymerase and hydrolase activities of *Bacillus subtilis* levansucrase can be separately modulated by site-directed mutagenesis. Biochem. J. **279**, 35–41

15 Simon, R., Priefer, U. and Puhler, A. (1983) A broad host range mobilization system for *in vivo* genetic engineering: transposon mutagenesis in Gram-negative bacteria. Bio/Technology **1**, 784–791

16 Hernandez, L., Arrieta, J., Betancourt, L., Falcon, V., Madrazo, J., Coego, A. and Menendez, C. (1999) Levansucrase from *Acetobacter diazotrophicus* SRT4 is secreted via periplasm by a signal-peptide-dependent pathway. Curr. Microbiol. **39**, 146–152

17 Arrieta, J., Hernandez, L., Coego, A., Suarez, V., Balmori, E., Menendez, C., Petit-Glatron, M. F., Chambert, R. and Selman-Housein, G. (1996) Molecular characterization of the levansucrase gene from the endophytic sugarcane bacterium *Acetobacter diazotrophicus* SRT4. Microbiology **142**, 1077–1085

18 Ditta, G., Schmidhauser, T., Yakobson, E., Lu, P., Liang, X. W., Finlay, D. R., Guiney, D. and Helinski, D. R. (1985) Plasmids related to the broad host range vector, pRK290, useful for gene cloning and for monitoring gene expression. Plasmid **13**, 149–153

19 Martinez-Fleites, C., Tarbouriech, N., Ortiz-Lombardia, M., Taylor, E., Rodriguez, A., Ramirez, R., Hernandez, L. and Davies, G. J. (2004) Crystallization and preliminary X-ray diffraction analysis of levansucrase (LsdA) from *Gluconacetobacter diazotrophicus* SRT4. Acta Crystallogr. Sect. D Biol. Crystallogr. **60**, 181–183

20 Collaborative Computational Project, Number 4 (1994) The CCP4 suite: programs for protein crystallography. Acta Crystallogr. Sect. D Biol. Crystallogr. **50**, 760–763

21 Navaza, J. (2001) Implementation of molecular replacement in AMoRe. Acta Crystallogr. Sect. D Biol. Crystallogr. **57**, 1367–1372

22 Brünger, A. T. (1992) The free R value: a novel statistical quantity for assessing the accuracy of crystal structures. Nature (London) **355**, 472–474

23 Brünger, A. T., Adams, P. D., Clore, G. M., DeLano, W. L., Gros, P., Grosse-Kunstleve, R. W., Jiang, J. S., Kuszewski, J., Nilges, M., Pannu, N. S. et al. (1998) Crystallography & NMR system: a new software suite for macromolecular structure determination. Acta Crystallogr. Sect. D Biol. Crystallogr. **54**, 905–921

24 McRee, D. E. (1999) XtalView/Xfit – a versatile program for manipulating atomic coordinates and electron density. J. Struct. Biol. **125**, 156–165

25 Murshudov, G. N. (1997) Refinement of macromolecular structures by the maximum-likelihood method. Acta Crystallogr. Sect. D Biol. Crystallogr. **53**, 240–255

26 Winn, M. D., Isupov, M. N. and Murshudov, G. N. (2001) Use of TLS parameters to model anisotropic displacements in macromolecular refinement. Acta Crystallogr. Sect. D Biol. Crystallogr. **57**, 122–133

27 Read, R. (1986) Improved Fourier coefficients for maps using phases from partial structures with errors. Acta Crystallogr. Sect. A Found. Crystallogr. **42**, 140–149

28 Ramachandran, G. N., Ramakrishnan, C. and Sasisekharan, V. (1963) Stereochemistry of polypeptide chain configurations. J. Mol. Biol. **7**, 95–99

29 Laskowski, R. A., Moss, D. S. and Thornton, J. M. (1993) Main-chain bond lengths and bond angles in protein structures. J. Mol. Biol. **231**, 1049–1067

30 Berman, H. M., Westbrook, J., Feng, Z., Gilliland, G., Bhat, T. N., Weissig, H., Shindyalov, I. N. and Bourne, P. E. (2000) The Protein Data Bank. Nucleic Acids Res. **28**, 235–242

31 Betancourt, L., Takao, T., Hernandez, L., Padron, G. and Shimonishi, Y. (1999) Structural characterization of *Acetobacter diazotropicus* levansucrase by matrix-assisted laser desorption/ionization mass spectrometry: identification of an N-terminal blocking group and a free-thiol cysteine residue. J. Mass Spectrom. **34**, 169–174

32 Beisel, H. G., Kawabata, S., Iwanaga, S., Huber, R. and Bode, W. (1999) Tachylectin-2: crystal structure of a specific GlcNAc/GalNAc-binding lectin involved in the innate immunity host defense of the Japanese horseshoe crab *Tachypleus tridentatus*. EMBO J. **18**, 2313–2322

33 Baker, S. C., Saunders, N. F., Willis, A. C., Ferguson, S. J., Hajdu, J. and Fulop, V. (1997) Cytochrome cd1 structure: unusual haem environments in a nitrite reductase and analysis of factors contributing to β-propeller folds. J. Mol. Biol. **269**, 440–455

34 Neer, E. J. and Smith, T. F. (1996) G protein heterodimers: new structures propel new questions. Cell **84**, 175–178

35 Paoli, M. (2001) Protein folds propelled by diversity. Prog. Biophys. Mol. Biol. **76**, 103–130

36 Hettwer, U., Gross, M. and Rudolph, K. (1995) Purification and characterization of an extracellular levansucrase from *Pseudomonas syringae* pv. *phaseolicola*. J. Bacteriol. **177**, 2834–2839

© 2005 Biochemical Society

37 Senthilkumar, V., Busby, S. J., Gunasekaran, P., Senthikumar, V. and Bushby, S. J. (2003) Serine substitution for cysteine residues in levansucrase selectively abolishes levan forming activity. Biotechnol. Lett. **25**, 1653–1656
38 Ohtsuka, K., Hino, S., Fukushima, T., Ozawa, O., Kanematsu, T. and Uchida, T. (1992) Characterization of levansucrase from *Rahnella aquatilis* Jcm-1683. Biosci. Biotechnol. Biochem. **56**, 1373–1377
39 Scales, W. R., Long, L. W. and Edwards, J. R. (1975) Purification and characterization of a glycosyltransferase complex from the culture broth of *Streptococcus mutans* FA1. Carbohydr. Res. **42**, 325–338
40 van Hijum, S. A., Szalowska, E., van der Maarel, M. J. and Dijkhuizen, L. (2004) Biochemical and molecular characterization of a levansucrase from *Lactobacillus reuteri.* Microbiology **150**, 621–630
41 van Hijum, S. A., van der Maarel, M. J. and Dijkhuizen, L. (2003) Kinetic properties of an inulosucrase from *Lactobacillus reuteri* 121. FEBS Lett. **534**, 207–210
42 Pons, T., Naumoff, D. G., Martinez-Fleites, C. and Hernandez, L. (2004) Three acidic residues are at the active site of a β-propeller architecture in glycoside hydrolase families 32, 43, 62, and 68. Proteins **54**, 424–432
43 Pons, T., Olmea, O., Chinea, G., Beldarrain, A., Marquez, G., Acosta, N., Rodriguez, L. and Valencia, A. (1998) Structural model for family 32 of glycosyl-hydrolase enzymes. Proteins **33**, 383–395
44 Yanase, H., Maeda, M., Hagiwara, E., Yagi, H., Taniguchi, K. and Okamoto, K. (2002) Identification of functionally important amino acid residues in *Zymomonas mobilis* levansucrase. J. Biochem. (Tokyo) **132**, 565–572
45 Engh, R. A. and Huber, R. (1991) Accurate bond and angle parameters for X-ray protein structure refinement. Acta Crystallogr. Sect. A Found. Crystallogr. **47**, 392–400
46 Cornish-Bowden, A. (1995) Analysis of Enzyme Kinetic Data, Oxford University Press, Oxford
47 DeLano, W. L. (2002) The PyMOL Molecular Graphics System, DeLano Scientific, San Carlos, CA
48 Kabsch, W. and Sander, C. (1983) Dictionary of protein secondary structure: pattern recognition of hydrogen-bonded and geometrical features. Biopolymers **22**, 2577–2637
49 Gouet, P., Courcelle, E., Stuart, D. I. and Metoz, F. (1999) ESPript: analysis of multiple sequence alignments in PostScript. Bioinformatics **15**, 305–308

Received 22 February 2005/26 April 2005; accepted 4 May 2005
Published as BJ Immediate Publication 4 May 2005, doi:10.1042/BJ20050324

© 2005 Biochemical Society